AUP1 transcriptionally activated by KDM5B reprograms lipid metabolism to promote the malignant progression of cervical cancer

YINGPING ZHU[1], WENJUAN YANG[2], XINYAN WANG[1] and MENGMENG CHEN[3]

[1]Department of Obstetrics and Gynecology, The First Affiliated Hospital of Zhejiang Chinese Medical University (Zhejiang Provincial Hospital of Chinese Medicine), Hangzhou, Zhejiang 310006, P.R. China; [2]First Clinical Medical College, Zhejiang Chinese Medical University, Hangzhou, Zhejiang 310059, P.R. China; [3]Gynecology and Obstetrics Department, Tenth People's Hospital, Tongji University School of Medicine, Shanghai 200072, P.R. China

Received July 8, 2024; Accepted September 9, 2024

DOI: 10.3892/ijo.2024.5695

Abstract. Cervical cancer is one of the reproductive malignancies threatening women's lives worldwide. In the present study, it was aimed to explore the role and mechanism of ancient ubiquitous protein 1 (AUP1) in cervical cancer. Through bioinformatics analysis, AUP1 expression in cervical cancer tissues and the correlation between AUP1 and the prognosis of patients were analyzed. AUP1 expression in several cervical cancer cell lines was detected. Following the co-transfection of short hairpin RNA specific to AUP1 with or without lysine demethylase 5B (KDM5B) overexpression plasmids in SiHa cells, the proliferation and apoptosis of SiHa cells were detected. Additionally, wound healing and Transwell assays were used to detect SiHa cell migration and invasion. Cellular lipid droplets level was detected using the Oil red O staining. Meantime, the levels of triglyceride, cholesterol, oxygen consumption rates and expression of lipid metabolism-related proteins were detected to assess the lipid metabolism in SiHa cells. Then, the luciferase reporter assay and ChIP assay were used to verify the binding between KDM5B and AUP1. Finally, the effects of AUP1 and KDM5B on the growth and lipid metabolism in SiHa tumor-bearing mice were measured. AUP1 was significantly upregulated in cervical cancer tissues and cells. AUP1 interference inhibited the malignant biological behaviors and lipid metabolism reprogramming of SiHa cells, which was blocked by KDM5B overexpression. Moreover, KDM5B could transcriptionally activate AUP1 and upregulate AUP1 expression. Furthermore, AUP1 knockdown transcriptionally regulated by KDM5B limited the tumor growth and suppressed the lipid metabolism reprogramming *in vivo*. Collectively, AUP1 could be transcriptionally activated by KDM5B to reprogram lipid metabolism, thereby promoting the progression of cervical cancer. These findings reveal possible therapeutic strategies in targeting metabolic pathways.

Correspondence to: Dr Mengmeng Chen, Gynecology and Obstetrics Department, Tenth People's Hospital, Tongji University School of Medicine, 301 Yan Chang Middle Road, Shanghai 200072, P.R. China
E-mail: chenmmmeng@163.com

Key words: ancient ubiquitous protein 1, lipid metabolism reprogramming, lysine demethylase 5B, proliferation, cervical cancer

Introduction

Cervical cancer, a prevalent gynecologic cancer, is the fourth leading cause of cancer-related death in women worldwide (1). According to American Cancer Society, there were 604,000 new cases of cervical cancer, and 342,000 women succumbed to cervical cancer in 2020 (2). In China, the incidence and mortality of patients with cervical cancer have gradually increased since 2000, making cervical cancer a public health issue of great concern (3). The persistent high-risk human papillomavirus (HPV) infection has been recognized as a leading cause of cervical cancer (4). Although widespread vaccination and screening have recently decreased the incidence of cervical cancer, they are not effective in women with precancerous lesions or cervical cancer (5). Hence, it is particularly necessary to uncover the underlying pathogenesis of cervical cancer and find novel targeted therapies for patients with cervical cancer.

It is well known that changes in cellular energy metabolism in the tumor microenvironment contributes to tumorigenicity and tumor progression (6). In recent years, lipid metabolism, which is a crucial part of tumor energy metabolism, has been recognized to play a significant role in the occurrence and metastasis of tumor cells (7,8). Cancer cells support the rapid proliferation, migration and invasion of tumor cells through activating lipid metabolism (9). Therefore, inhibition of abnormal lipid metabolic processes in cancer cells may be an important strategy for cancer therapy (7). Of note, lipid metabolism has been considered as a new therapeutic target for cervical cancer, and an increasing number of researchers have analyzed the potential link between lipid metabolism reprogramming and the molecular mechanism of cervical cancer pathogenesis (10-12).

Ancient ubiquitous protein 1 (AUP1) located on human chromosome 2p13 is initially found to be a protein that contains 410 amino acids (13). It is noted that AUP1 plays a significant role in lipid droplet degradation through interaction with the Ubiquitin Conjugating Enzyme E2 G2 (UBE2G2) to ligase the ubiquitin, then proceed to the lipophagy pathway (14). As reported, AUP1 can directly interfere with tumor progression by regulating a series of complex lipid metabolic cascades (15). For instance, AUP1 knockdown markedly decreases the contents of intracellular triglyceride (TG) and cholesterol (CHOL) (15). AUP1 can induce lipid accumulation in cancer cells by facilitating the *de novo* synthesis of fatty acids (15). The HumanTFDB database was used to predict the upstream transcription factors that could transcriptionally regulate AUP1 expression, and found that lysine demethylase 5B (KDM5B) could bind to the promotor region of AUP1. KDM5B, which catalyzes the demethylation of histone 3 lysine 4, is important for embryonic stem cell differentiation (16). It is addressed that KDM5B is also overexpressed, amplified, or mutated in numerous cancer types (17). As a new regulator involved in lipid metabolism reprogramming, KDM5B facilities the proliferation and migration of breast cancer cells via AMPK-mediated lipid metabolism reprogramming (18). Importantly, KDM5B is significantly upregulated in cervical cancer, and KDM5B knockdown suppresses the growth of cervical cancer cells (19). Accordingly, it was hypothesized that AUP1 transcriptionally activated by KDM5B reprogramed lipid metabolism to accelerate the malignant progression of cervical cancer.

In the present study, AUP1 expression in cervical cancer tissues and the correlation between AUP1 expression and prognosis of patients with cervical cancer were analyzed using bioinformatic tools. The effects of AUP1 silencing on the malignant biological behaviors and lipid metabolism of cervical cancer cells and transplantation tumor model were explored. Further experiments investigated the regulation between AUP1 and KDM5B. The current findings may reveal a novel mechanism by which AUP1 contributes to tumorigenesis in cervical cancer.

Materials and methods

Bioinformatics analysis. AUP1 expression in normal cervical tissues (Normal; n=3) and tissues of patients with primary cervical squamous cell carcinoma (CESC; n=305) was analyzed using UALCAN database (https://ualcan.path.uab.edu/) (20). The association between AUP1 expression and the prognosis of patients with cervical cancer was detected using Kaplan-Meier Plotter database (http://www.kmplot.com/) (21). HumanTFDB database (http://bioinfo.life.hust.edu.cn/HumanTFDB#!/) was used to predict the upstream transcription factors that could transcriptionally activate AUP1 (22).

Cell culture. The human immortalized cervical epithelial cell line (H8) was supplied from BLUEFBIO (cat. no. BFN607200572; http://www.bluefcell.com/sy). Four human cervical cancer cells lines [SiHa (cat. no. BNCC337881), Caski (cat. no. BNCC354385), HeLa (cat. no. BNCC342189) and C33A (cat. no. BNCC354329) cells)] were obtained from BeNa Culture Collection. Cells were incubated in Dulbecco's Modified Eagle's Medium (DMEM; Gibco; Thermo Fisher Scientific, Inc.) containing 10% fetal bovine serum (FBS; HyClone; Cytiva) in a humidified atmosphere with 5% CO_2 at 37˚C.

Transfection. To silence AUP1 or overexpress KDM5B, short hairpin RNA (shRNA) specific to AUP1 (sh-AUP1-1, 5'-CGC TTCAGTTCCTGGCCATTT-3';sh-AUP1-2,5'-CTCAGAGAG TCAAGGAAGTTT-3'), KDM5B (sh-KDM5B-1, 5'-GTCTGT CCTTGCACATATTAC-3'; sh-KDM5B-2, 5'-GTTCCTGTC CTCCTTACAAAT-3'), the negative control (sh-NC, 5'-GAG CGATTCTCCTGCAGCATG-3'), KDM5B overexpressing plasmid (oe-KDM5B) and the empty vector plasmid (oe-NC) were designed and synthesized by Shanghai GenePharma Co., Ltd. These recombinants (50 nmol/l) were transfected into SiHa cells ($3x10^5$ cells/well) using Lipofectamine 3000 reagent (Invitrogen; Thermo Fisher Scientific, Inc.) for 48 h at 37˚C according to the manufacturer's protocol. After transfection for 48 h, SiHa cells were harvested for follow-up experiments. The transfection efficiencies were analyzed using reverse transcription-quantitative PCR (RT-qPCR) and western immunoblot analysis.

Test for cell viability. Cell Counting Kit-8 (CCK-8; Beyotime Institute of Biotechnology) assay was used to detect SiHa cell viability after transfection. The transfected SiHa cells were seeded into 96-well plates ($2x10^4$ cells/well). After cell incubation for 24, 48 and 72 h at 37˚C, 10 μl CCK-8 buffer was added to each well and cells were incubated for additional 4 h. The absorbance was recorded at 450 nm using a microplate reader (Bio-Rad Laboratories, Inc.).

Measurement of colony formation. After transfection, SiHa cells (500 cells/well) were plated onto 6-well plate and incubated for 2 weeks at 37˚C with 5% CO_2. Colonies were fixed with 4% paraformaldehyde for 20 min at room temperature and stained with 1% crystal violet for 15 min at room temperature. The colony formation (>50 cells) was observed and the images were obtained using a light microscope (Olympus Corporation).

5-ethynyl-2'-deoxyuridine (EdU) staining. The proliferation of SiHa cells after transfection was assessed using an EDU kit (Beyotime Institute of Biotechnology). SiHa cells were cultured in a 12-well plate at 37˚C with 5% CO_2 until 80% confluence was achieved. Cells were stained with EdU solution for 3 h at 37˚C and nuclei were labeled with 4',6-diamidino-2-phenylindole (DAPI; 5 mg/ml, 1:1,000) for 10 min at room temperature. The cell proliferation was detected using a fluorescence microscope (Olympus Corporation).

Apoptosis assessment. An Annexin V-FITC Apoptosis Detection Kit (Beyotime Institute of Biotechnology) was used to detect the apoptosis of SiHa cells. SiHa cells ($2x10^6$ cells) were resuspended in Annexin-binding buffer. After that, SiHa cells were stained with 5 μl Annexin V-FITC and 10 μl PI for 15 min at room temperature. Cell apoptosis was analyzed with a flow cytometer (BD FACS Caliber; BD Biosciences) and the percentage of apoptotic cells was calculated with FlowJo V7 software (Tree Star, Inc.).

Wound scratch healing assay. The transfected SiHa cells were seeded in the 6-well plates and cultured at 37˚C with 5% CO_2. When the cells were cultured to 90% confluence, a wound was created using a 20-μl pipette tip through the cell monolayer. Afterwards, cells were washed with PBS for three times and maintained in serum-starved DMEM for 24 h at 37˚C. The images of wounds were recorded at 0 and 24 h by a light microscope (Olympus Corporation). The wound healing ratio was determined by ImageJ software. The migration rate was calculated based on the formula: (Wound width at 0 h-wound width at 24 h)/wound width at 0 h x100%.

Transwell assay. After cell transfection, Transwell chambers (8-μm pores; Corning, Inc.) pre-coated with Matrigel (BD Biosciences) overnight at 37˚C were used to detect the invasion of SiHa cells. SiHa cells ($1x10^5$ cells) suspended in serum-free DMEM were added to the upper chambers. DMEM with 10% FBS was added into the lower chamber as a chemoattractant. After incubating for 48 h in the incubator, SiHa cells were fixed with 4% paraformaldehyde for 10 min at room temperature and stained with crystal violet for 15 min at room temperature. A light microscope (Olympus Corporation) was used for observation and then the number of invasive cells was calculated using ImageJ 1.8.0 software (National Institutes of Health).

Detection of TG and CHOL contents. The transfected SiHa cells were lysed with ice-cold RIPA buffer and centrifuged (600 x g) for 10 min at 4˚C to obtain supernatant. The contents of TG (cat. no. A110-1-1) and CHOL (cat. no. A111-1-1) in the supernatant were analyzed according to the manufacturer's protocol using the commercial kits (Nanjing Jiancheng Bioengineering Institute). The absorbance at 500 nm was detected under a microplate reader (Bio-Rad Laboratories, Inc.).

Assessment of oxygen consumption rates (OCR). Through Seahorse XF Cell Mito Stress Test Kit in the Seahorse XFe96 analyzer (Seahorse Bioscience), OCR (pmol/min) was calculated according to the manufacturer's protocol. The data were analyzed using Seahorse XF-96 Wave software.

Luciferase reporter assay. By using HumanTFDB database, KDM5B was predicted to have the putative binding site on AUP1 promoter. Cells were co-transfected with pGL3-basic vectors (Promega Corporation) containing the wild-type (WT) or mutant (MUT) AUP1 promoter sequence, oe-KDM5B and oe-NC using Lipofectamine 3000 reagent (Invitrogen; Thermo Fisher Scientific, Inc.). After transfection for 48 h, the Dual Luciferase Reporter Gene Assay Kit (Beyotime Institute of Biotechnology) was used to analyze the luciferase activity. Luciferase activity was normalized to *Renilla* luciferase.

Chromatin immunoprecipitation (ChIP) assay. ChIP assay was performed using the ChIP kit (Absin). SiHa cells were collected with ice-cold RIPA buffer (Beyotime Institute of Biotechnology) and cross-linked with 1% formaldehyde for 10 min at room temperature. Chromatin cross-linking was stopped by glycine. The 100 μl lysates were incubated with anti-KDM5B (5 μg; cat. no. 15327S; Cell Signaling Technology, Inc.) or anti-IgG (1.5 μg; cat. no. 30000-0-AP; Proteintech Group, Inc.) antibody for 2 h at 4˚C. Protein A agarose was supplemented to precipitate the endogenous DNA-protein complex. Subsequent to transient centrifugation at 6,500 x g for 1 min at 4˚C, the supernatant was discarded and the non-specific complexes were washed. The purified DNA fragments were subjected to PCR analysis.

Tumorigenicity assays in nude mice. A total of 20 female BALB/c nude mice (6 weeks, 18-20 g; Hangzhou Ziyuan Laboratory Animal Technology Co., Ltd.) were maintained in a standardized SPF environment with 12/12-h light-dark cycle, 21-23˚C and a relative humidity of 60-65%, with *ad libitum* access to food and water. A total of $1x10^7$ SiHa cells transfected with sh-AUP1, sh-AUP1 + oe-NC or sh-AUP1 + oe-KDM5B were resuspended in 200 μl PBS and subcutaneously injected into the right flank of BALB/c nude mice. Tumor volume calculated as $(width)^2$ length/2 was monitored every two days from day 6 after injection. On the 24th day, all mice were sacrificed by intraperitoneal injection of pentobarbital sodium (150 mg/kg), and tumor tissues were collected and images were captured. All animal studies were approved by the Laboratory Animal Ethics Committee of The First Affiliated Hospital of Zhejiang Chinese Medical University (approval no. HB2005007; Hangzhou, China).

Immunofluorescence staining. The tumorous tissue samples collected from SiHa tumor-bearing mice were fixed in 4% paraformaldehyde for 24 h at room temperature and then embedded in paraffin. The paraffin-embedded tissue sections (5 μm thick) were conventionally dewaxed with xylene and rehydrated with gradient ethanol. The sections were permeabilized with 0.1% Triton X-100, and then blocked by 5% bovine serum albumin (BSA; Beyotime Institute of Biotechnology) for 1 h at room temperature. Sections were incubated with anti-Ki67 primary antibody (2 μg/ml; cat. no. ab16667; Abcam) at 4˚C overnight. After washing with PBS for three times, the sections were incubated with fluorescence-labeled secondary antibody (1:1,000; cat. no. 8890S; Cell Signaling Technology, Inc.) for 1 h at 37˚C. Nuclei were counterstained with DAPI (5 mg/ml, 1:1,000) for 15 min at room temperature in the dark. Images were captured using a fluorescence microscope (Olympus Corporation).

TUNEL staining. The tumorous tissue samples collected from SiHa tumor-bearing mice were fixed in 4% paraformaldehyde for 24 h at room temperature and then embedded in paraffin. The paraffin-embedded tissue sections (5-μm thick) were dewaxed. The endogenous peroxidase activity in sections were blocked with 3% H_2O_2. The sections were incubated with TUNEL reaction mixture (50 μl) for 1 h at room temperature. The nuclei were counterstained with DAPI (5 mg/ml, 1:1,000) for 15 min at room temperature. A total of three random fields of view were captured with a fluorescence microscope (Olympus Corporation) and the percentage of TUNEL-positive cells was calculated.

Oil red O staining. $2x10^5$ SiHa cells were fixed with 4% paraformaldehyde for 15 min at room temperature and then rinsed in isopropanol. Subsequently, the cells were stained with Oil Red O working solution for 30 min at room temperature.

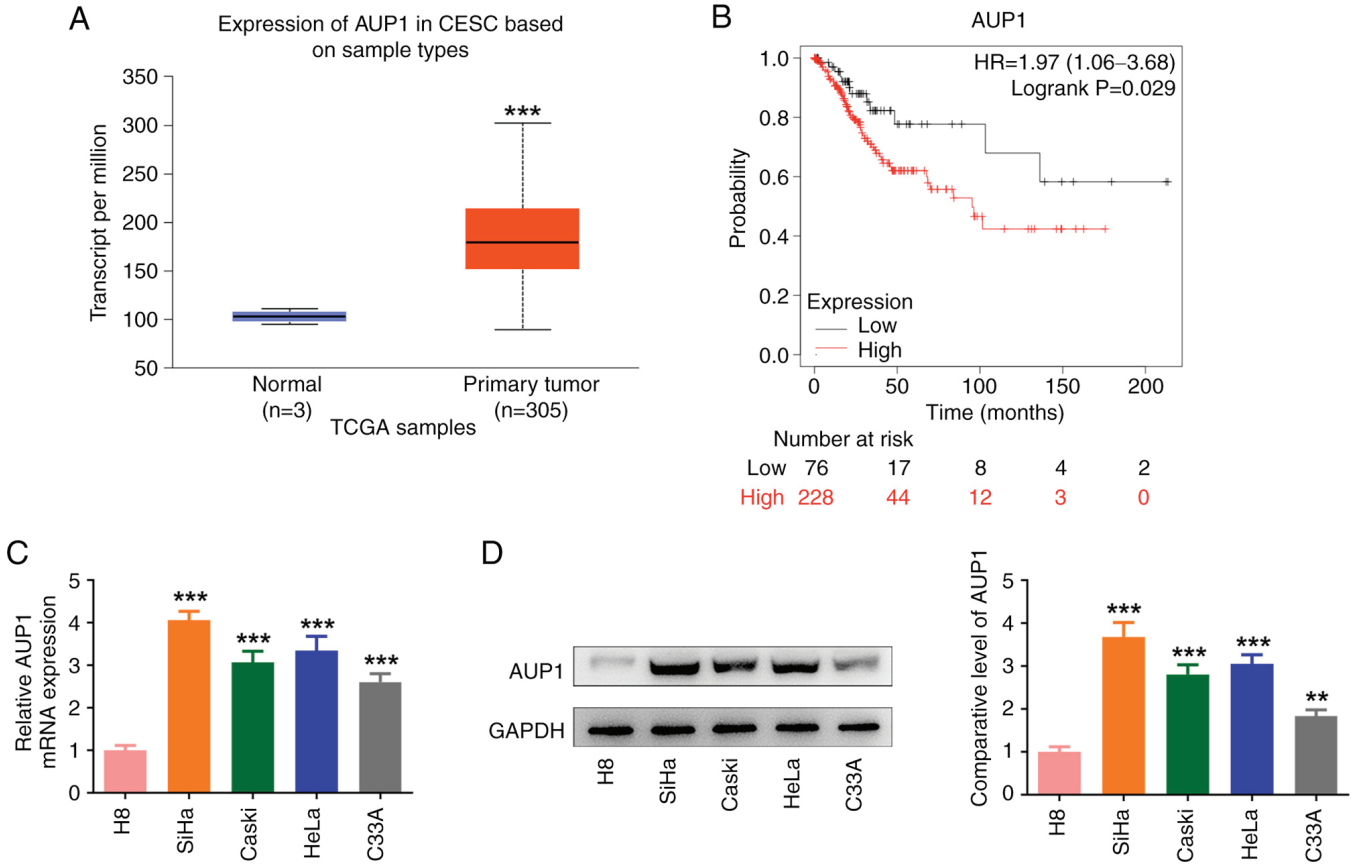

Figure 1. AUP1 expression is significantly upregulated in cervical cancer tissues and cells. (A) AUP1 expression in normal cervical tissues (Normal; n=3) and tissues of patients with primary CESC (n=305) was analyzed using UALCAN database. ***P<0.001 vs. Normal group. (B) The association between AUP1 expression and the prognosis of patients with cervical cancer was analyzed using Kaplan-Meier Plotter database. (C) Reverse transcription-quantitative PCR and (D) western immunoblot analysis were used to analyze AUP1 expression in four cervical cancer cell lines (SiHa, Caski, HeLa and C33A cells) and the human immortalized cervical epithelial cell line (H8 cells). **P<0.01 and ***P<0.001 vs. H8 group. AUP1, ancient ubiquitous protein 1; CESC, cervical squamous cell carcinoma.

For tumorous tissue, the tissue sections (5 μm thick) were embedded with paraffin, dewaxed and stained by Oil Red O dye liquor for 30 min at room temperature. After washing with distilled water, the stained SiHa cells and tissue sections were counter-stained by haematoxylin for 1 min at room temperature. The images were observed and captured under a light microscope (Olympus Corporation).

RT-qPCR. Total RNA was isolated using TRIzol® reagent (Invitrogen; Thermo Fisher Scientific, Inc.). The PrimeScript RT reagent kit (Takara Bio, Inc.) was used to amplify the synthesized cDNA according to the manufacturer's protocol. Reactions were run on an ABI 7500 Real-Time PCR System with the SYBR Green PCR Master Mix (Takara Bio, Inc.) according to the manufacturer's protocol. The following thermocycling conditions were used: Initial denaturation at 95˚C for 10 min; followed by 35 cycles of denaturation at 95˚C for 15 sec, annealing at 60˚C for 1 min and extension of 10 min at 65˚C. PCR data were analyzed using $2^{-\Delta\Delta Cq}$ method (23). Comparative threshold values were normalized to GAPDH. The following primer pairs were used for qPCR: AUP1 forward, 5'-CTCAGCCAACAGCCCTAACA-3' and reverse, 5'-GGGTGCCATCCTGTTCCTTT-3'; KDM5B forward, 5'-CAGCCTGCGGTGATGGAG-3' and reverse, 5'-TGGATGAAAGCGAAGGGGTC-3'; GAPDH forward, 5'-AATGGGCAGCCGTTAGGAAA-3' and reverse, 5'-GCGCCCAATACGACCAAATC-3'.

Western immunoblot analysis. Cells or tumorous tissues were lysed with ice-cold RIPA buffer (Beyotime Institute of Biotechnology). Protein concentrations were estimated using the Bradford assay. Separated by 10% SDS-PGE gels, equal amounts of proteins (40 μg per lane) were then transferred onto PVDF membranes. The membranes were blocked with 5% BSA for 1 h at room temperature, and then incubated with primary antibodies at 4˚C overnight. Then, the membrane was incubated with the HRP-conjugated secondary antibody (1:10,000; cat. no. 7074P2; Cell Signaling Technology, Inc.) at room temperature for 1 h. The protein bands were visualized with the enhanced chemiluminescence and the protein density was quantified using ImageJ software. GAPDH or LaminB1 was used for the control loading. Anti-AUP1 (1:1,000; cat. no. 35055S), anti-proliferating cell nuclear antigen (PCNA; 1:1,000; cat. no. 13110T), anti-B-cell chronic lymphocytic leukemia/lymphoma-2 (Bcl-2; 1:1,000; cat. no. 3498T), anti-Bcl-2-associated X protein (Bax; 1:1,000; cat. no. 2772T), anti-matrix metalloproteinases 2 (MMP2; 1:1,000; cat. no. 87809S), anti-MMP9 (1:1,000; cat. no. 13667T), anti-KDM5B (1:1,000; cat. no. 15327S), anti-LaminB1 (1:1,000; cat. no. 13435S) and

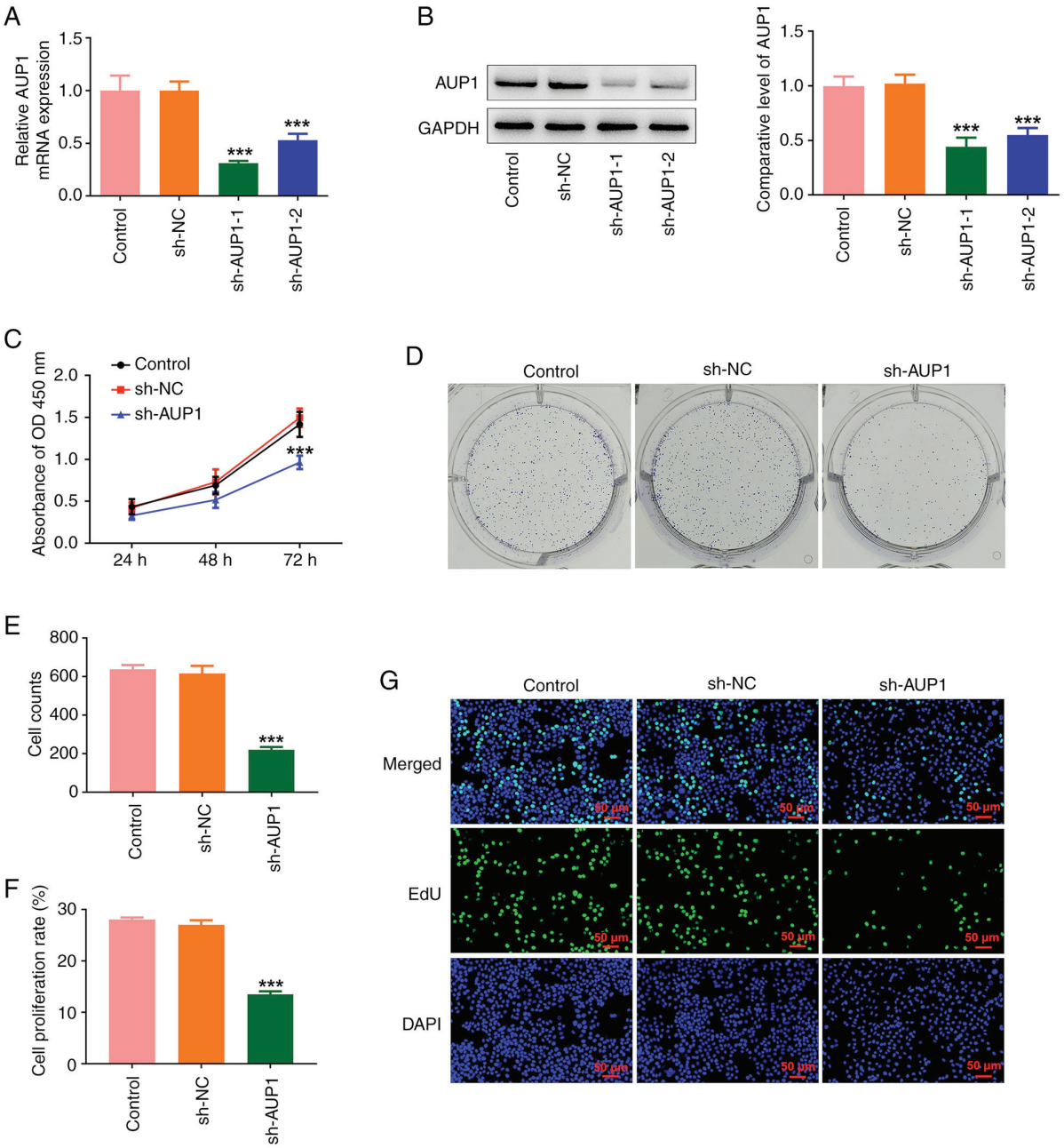

Figure 2. AUP1 interference inhibits the proliferation of cervical cancer cells. (A) Reverse transcription-quantitative PCR and (B) western immunoblot analysis were used to examine AUP1 expression in SiHa cells after transfection with sh-AUP1-1/2. (C) Cell Counting Kit-8 assay measured the viability of SiHa cells. (D and E) Cell proliferation was assessed by colony formation assay. (F and G) EdU staining detected the proliferation of SiHa cells. ***P<0.001 vs. sh-NC group. AUP1, ancient ubiquitous protein 1; EdU, 5-ethynyl-2'-deoxyuridine; sh-, short hairpin; NC, negative control.

anti-GAPDH (1:1,000; cat. no. 2118T) antibodies were acquired from Cell Signaling Technology, Inc. Anti-Ki67 (1:100) and anti-carnitine palmitoyltransferase IA (CPT1A; 1:1,000; cat. no. ab234111; Abcam) antibodies were also used. Anti-StAR-related lipid transfer domain containing 5 (STARD5; 1:1,000; cat. no. 10487-1-AP), anti-AMP-activated protein kinase subunit alpha 2 (PRKAA2; 1:500; cat. no. 18167-1-AP) and anti-monoglyceride lipase (MGLL; 1:500; cat. no. 14986-1-AP) antibodies were obtained from Proteintech Group, Inc.

Statistical analysis. All experiments were repeated at least three times independently. Data were expressed as the mean ± standard deviation (SD) and analyzed with GraphPad 8.0 software (GraphPad Software Inc.; Dotmatics). Differences among multiple groups were analyzed by one-way ANOVA followed by post-hoc Tukey's analysis. P<0.05 was considered to indicate a statistically significant significance.

Results

AUP1 expression is significantly upregulated in cervical cancer tissues and cells. UALCAN database was used to analyze AUP1 expression in normal cervical tissues and tissues of patients with primary CESC. It was found that AUP1 was highly expressed in cervical cancer tissues compared with normal cervical tissues

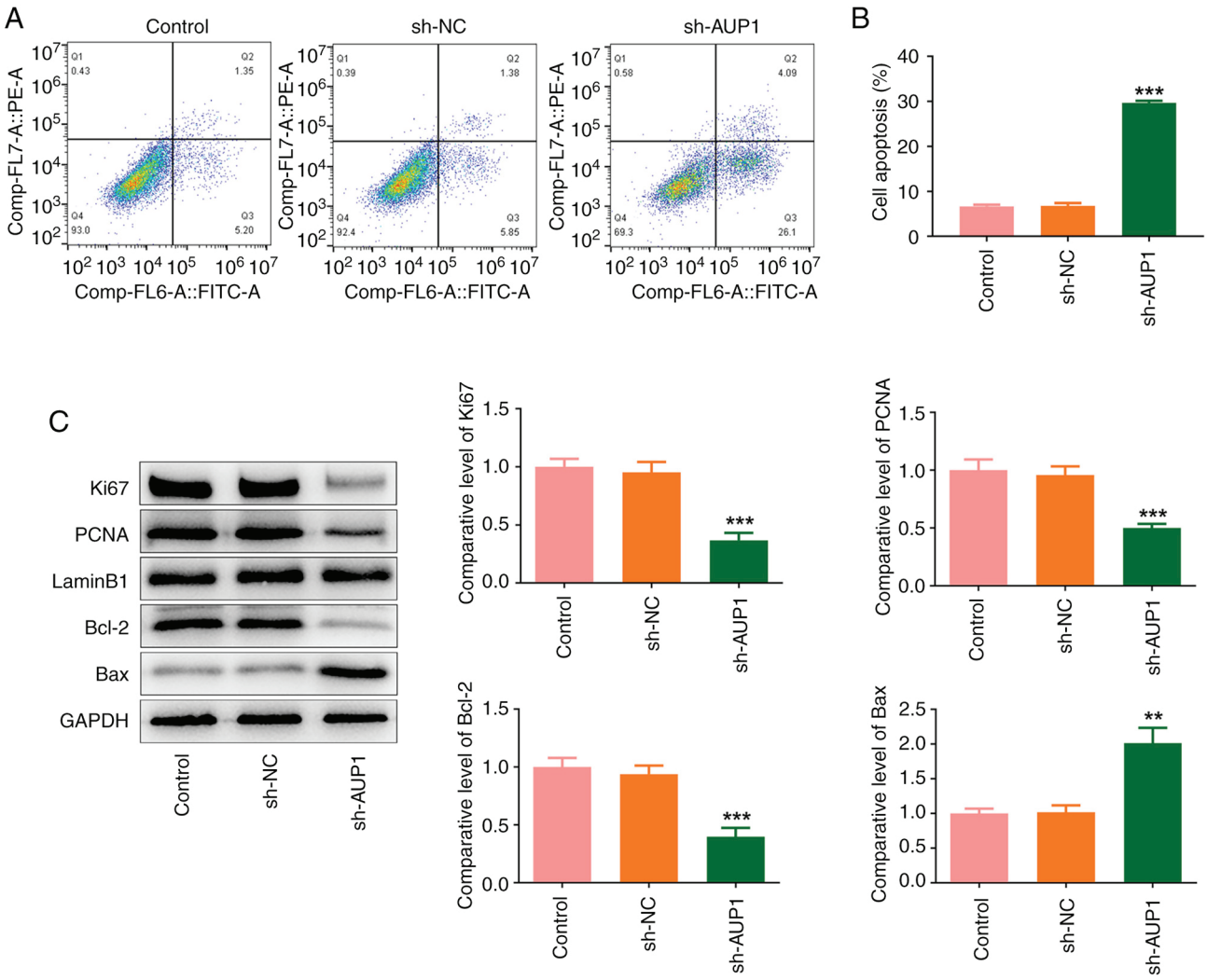

Figure 3. AUP1 interference facilitates the apoptosis of cervical cancer cells. (A and B) SiHa cell apoptosis was detected using flow cytometric analysis. (C) Western immunoblot analysis measured Ki67, PCNA, Bcl-2 and Bax expression in SiHa cells. **P<0.01 and ***P<0.001 vs. sh-NC group. AUP1, ancient ubiquitous protein 1; PCNA, proliferating cell nuclear antigen; sh-, short hairpin; NC, negative control.

(Fig. 1A). According to Kaplan-Meier Plotter database, higher AUP1 expression in patients with cervical cancer was associated with poorer prognosis (Fig. 1B). The subsequent RT-qPCR and western immunoblot analysis indicated that AUP1 was abnormally upregulated in cervical cancer cells lines (SiHa, Caski, HeLa and C33A cells) compared with the human immortalized cervical epithelial cell line (H8) (Fig. 1C and D). Of note, SiHa cells exhibited the highest AUP1 expression compared with the other three cervical cancer cells lines. Hence, SiHa cells were chosen for the following functional experiments. The present data suggested the abnormally high expression of AUP1 in cervical cancer tissues and cells.

AUP1 interference inhibits the malignant biological behaviors of cervical cancer cells. To study the role of AUP1 interference in the malignant biological behaviors of cervical cancer cells, sh-AUP1-1/2 was transfected into SiHa cells to knock down AUP1 expression. Compared with the sh-NC group, AUP1 expression was significantly decreased in sh-AUP1-1 and sh-AUP1-2 groups (Fig. 2A and B). It was also found that AUP1 expression in sh-AUP1-1 group was lower than that of sh-AUP1-2 group. Therefore, SiHa cells transfected with sh-AUP1-1 were selected for following experiments. Cell proliferation was tested using CCK-8, colony formation and EdU staining. As shown in Fig. 2C-G, AUP1 interference significantly inhibited the proliferation of SiHa cells, reduced the colony formation and decreased EdU fluorescence intensity. In addition, AUP1 knockdown significantly increased the percentage of apoptotic SiHa cells compared with the sh-NC group (Fig. 3A and B). Ki67, PCNA and Bcl-2 expression was significantly downregulated while Bax expression was upregulated in AUP1-silenced SiHa cells (Fig. 3C). Besides, MMPs are the main proteases involved in tumor cell metastasis migration and invasion (24). Among them, MMP2 and MMP9 are key enzymes that involved in the metastatic process of cervical cancer (25,26). As exhibited in Fig. 4A-C, AUP1 deficiency significantly attenuated the migration and invasion of SiHa cells, accompanied by decreased MMP2 and MMP9 expression. Collectively, the aforementioned results suggested that AUP1 interference suppressed the proliferation and induced the apoptosis of cervical cancer cells.

AUP1 interference inhibits the lipid metabolism reprogramming of cervical cancer cells. The alteration of lipid metabolism

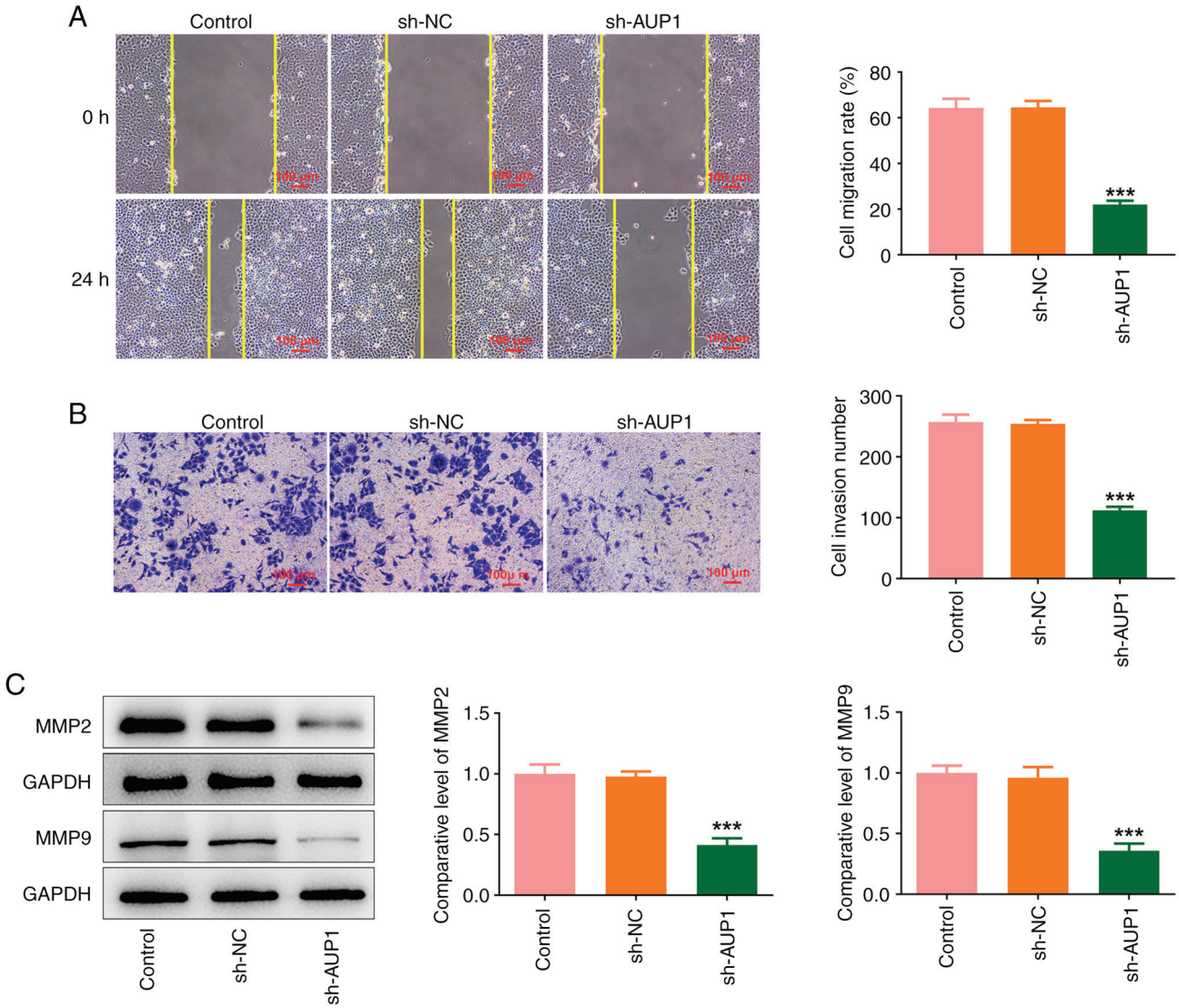

Figure 4. AUP1 interference inhibits the migration and invasion of cervical cancer cells. (A) Wound healing assay was used to detect the migration of SiHa cells. (B) The invasion of SiHa cells was detected by Transwell assay. (C) Western immunoblot analysis was used to identify MMP2 and MMP9 expression in SiHa cells. ***P<0.001 vs. sh-NC group. AUP1, ancient ubiquitous protein 1; MMP, matrix metalloproteinase; sh-, short hairpin; NC, negative control.

has been known as a crucial process in various cancers and lipid metabolism has been considered as a new therapeutic target for cervical cancer (12,27). The effect of AUP1 interference on lipid metabolism was analyzed in the subsequent assays. Results of Oil red O staining indicated that AUP1 interference significantly decreased lipid droplets, cellular TG and CHOL contents in SiHa cells (Fig. 5A-C). OCR is an indicator of mitochondrial respiration (28). As demonstrated in Fig. 5D, compared with the sh-NC group, sh-AUP1 significantly inhibited the OCR of SiHa cells. The further western immunoblot analysis detected the crucial enzymes involved in the regulation of lipid metabolism (15,29,30) and demonstrated that AUP1 loss-of-function increased CPT1A, STARD5 and PRKAA2 expression while reduced MGLL expression in SiHa cells (Fig. 5E). These data confirmed that AUP1 interference could inhibit the lipid metabolism reprogramming of cervical cancer cells.

KDM5B transcriptionally activates AUP1 and upregulates AUP1 expression in cervical cancer cells. To study the potential mechanism of AUP1 in regulating the malignant biological behaviors of cervical cancer cells, HumanTFDB database was used to predict the upstream transcription factors that could transcriptionally regulate AUP1 expression, and it was found that KDM5B could bind to the promotor region of AUP1 (Fig. 6A). Compared with the H8 cells, AUP1 expression was significantly upregulated in SiHa cells (Fig. 6B and C). Then, KDM5B was overexpressed or silenced by transfection with oe-KDM5B or sh-KDM5B-1/2. As revealed in Fig. 6D and E, transfection of oe-KDM5B significantly increased KDM5B expression and sh-KDM5B-1/2 significantly reduced KDM5B expression. SiHa cells transfected with sh-KDM5B-1 were chosen for follow-up experiments due to its improved transfection efficiency. Luciferase reporter assay revealed that oe-KDM5B significantly increased the promotor activity of AUP1 compared with the oe-NC group (Fig. 6F). Results of ChIP assay also confirmed the binding of KDM5B to AUP1 promoter (Fig. 6G). Moreover, KDM5B overexpression significantly upregulated AUP1 expression and KDM5B knockdown significantly downregulated AUP1 expression in SiHa cells

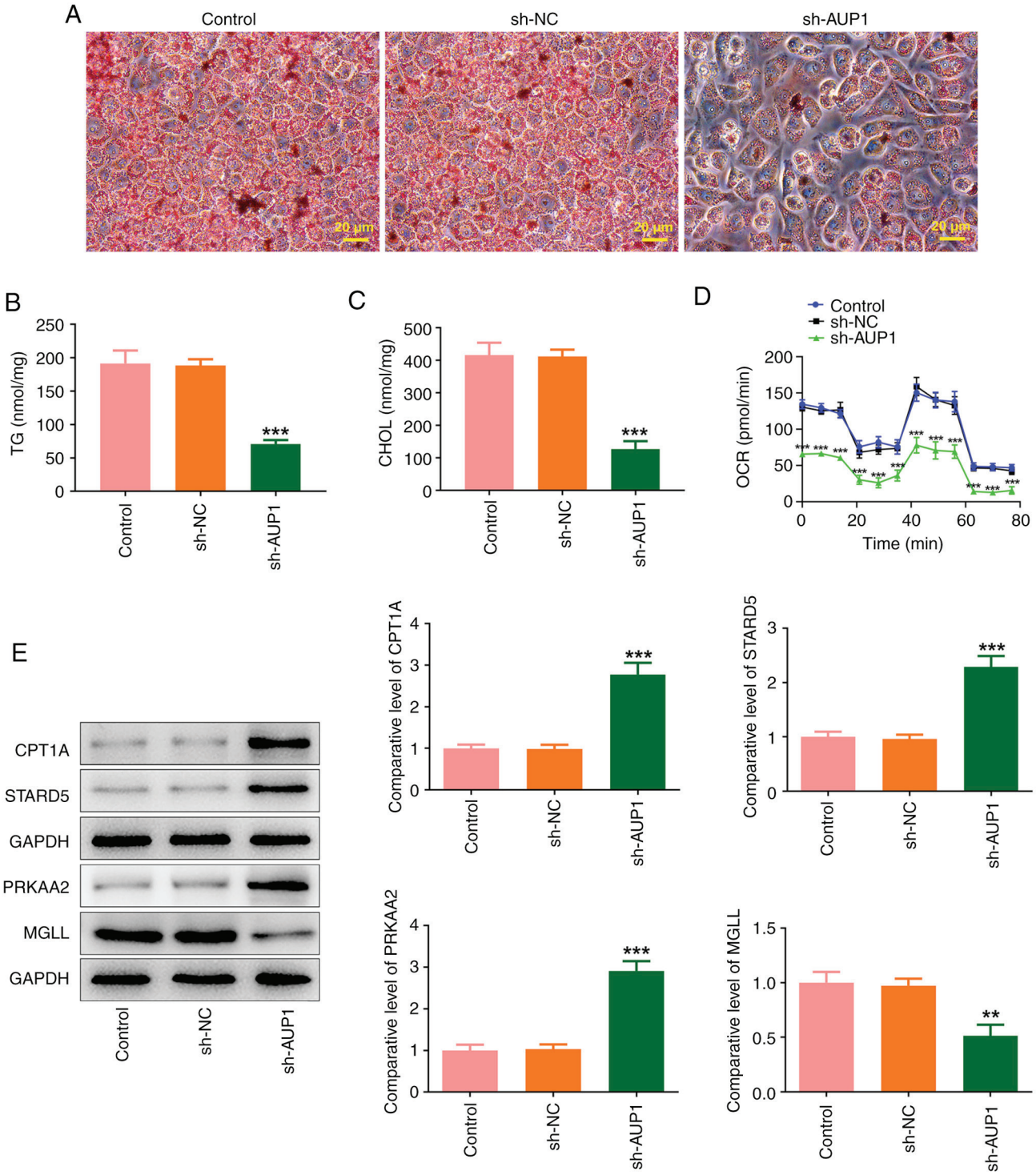

Figure 5. AUP1 interference inhibits the lipid metabolism reprogramming of cervical cancer cells. (A) Oil red O staining was used to detect lipid droplets in SiHa cells. The contents of (B) TG and (C) CHOL in SiHa cells were analyzed using the corresponding kits. (D) OCR in SiHa cells was detected using the Seahorse XF Cell Mito Stress Test Kit. (E) The expression of proteins related to lipid metabolism was detected using western immunoblot analysis. **P<0.01 and ***P<0.001 vs. sh-NC group. AUP1, ancient ubiquitous protein 1; TG, triglyceride; CHOL, cholesterol; OCR, oxygen consumption rates; sh-, short hairpin; NC, negative control; CPT1A, carnitine palmitoyltransferase IA; STARD5, StAR-related lipid transfer domain containing 5; MGLL, monoglyceride lipase.

(Fig. 6H and I). These results demonstrated that KDM5B could transcriptionally activate AUP1 and upregulate AUP1 expression in cervical cancer cells.

KDM5B overexpression blocks the inhibitory effects of AUP1 silencing on the malignant biological behaviors of cervical cancer cells. The rescue experiments were conducted through the co-transfection with sh-AUP1 and oe-KDM5B into SiHa cells. As depicted in Fig. 7A-E, KDM5B overexpression significantly promoted the proliferation of SiHa cells compared with the sh-AUP1 + oe-NC group. Additionally, compared with the sh-AUP1 + oe-NC group, the apoptotic percentage of SiHa cells was significantly decreased after the transfection with sh-AUP1 and oe-KDM5B (Fig. 7F and G).

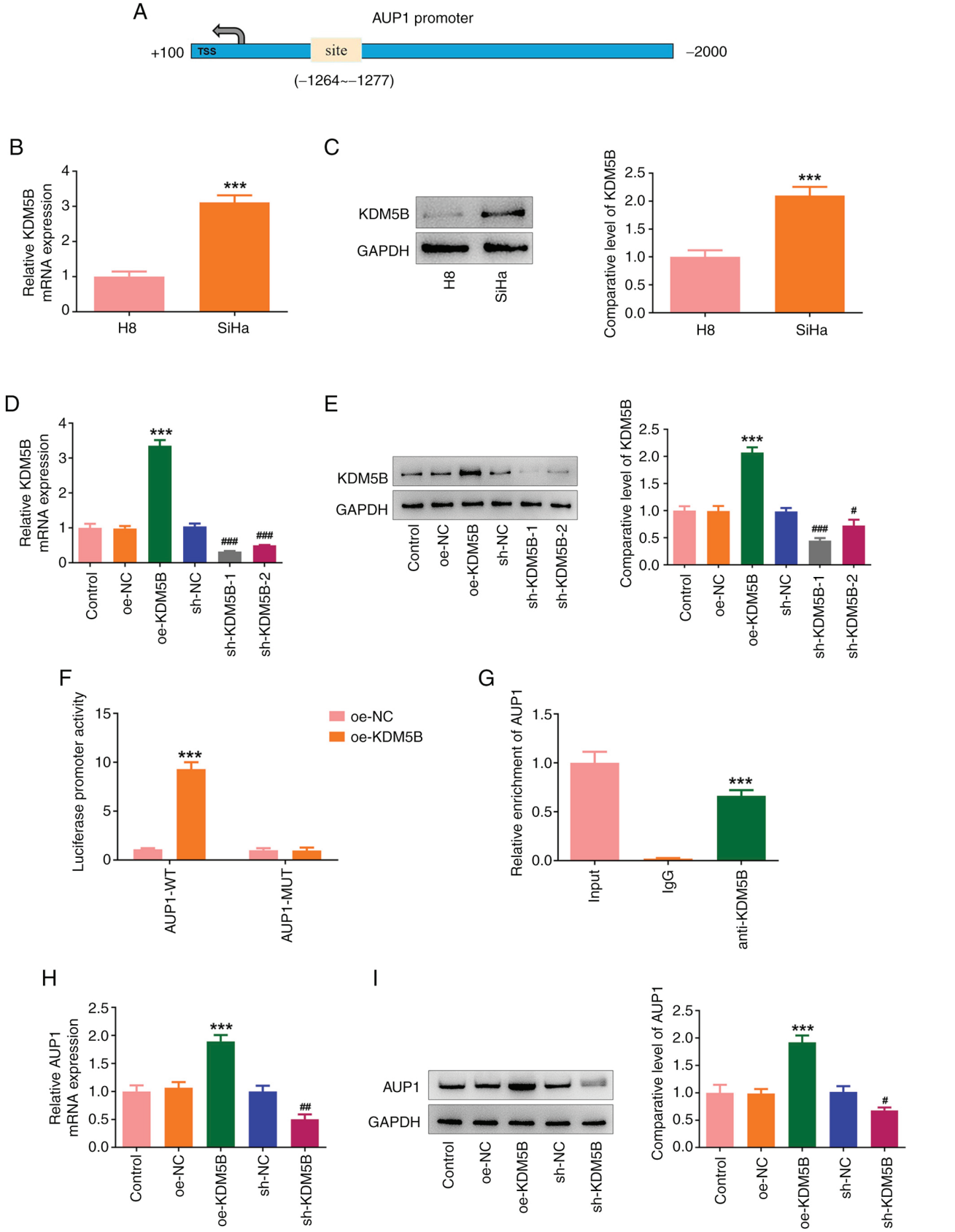

Figure 6. KDM5B could transcriptionally activate AUP1 and upregulate AUP1 expression in cervical cancer cells. (A) The putative KDM5B-binding site on the AUP1 promoter was predicated by the HumanTFDB database. (B) RT-qPCR and (C) western immunoblot analysis were used to measure KDM5B expression in H8 cells and SiHa cells. ***P<0.001 vs. H8 group. (D) RT-qPCR and (E) western immunoblot analysis analyzed KDM5B expression in SiHa cells after transfection with oe-KDM5B or sh-KDM5B-1/2. ***P<0.001 vs. oe-NC group; #P<0.05 and ###P<0.001 vs. sh-NC group. The binding of KDM5B on AUP1 promoter site was verified using (F) luciferase reporter assay and (G) chromatin immunoprecipitation assay. ***P<0.001 vs. oe-NC group or IgG group. (H) RT-qPCR and (I) western immunoblot analysis were used to analyze KDM5B expression in SiHa cells after transfection with oe-KDM5B or sh-KDM5B. ***P<0.001 vs. oe-NC group; #P<0.05 and ##P<0.01 vs. sh-NC group. KDM5B, lysine demethylase 5B; AUP1, ancient ubiquitous protein 1; RT-qPCR, reverse transcription-quantitative PCR; sh-, short hairpin; NC, negative control; oe-overexpressing; WT, wild-type; MUT, mutant.

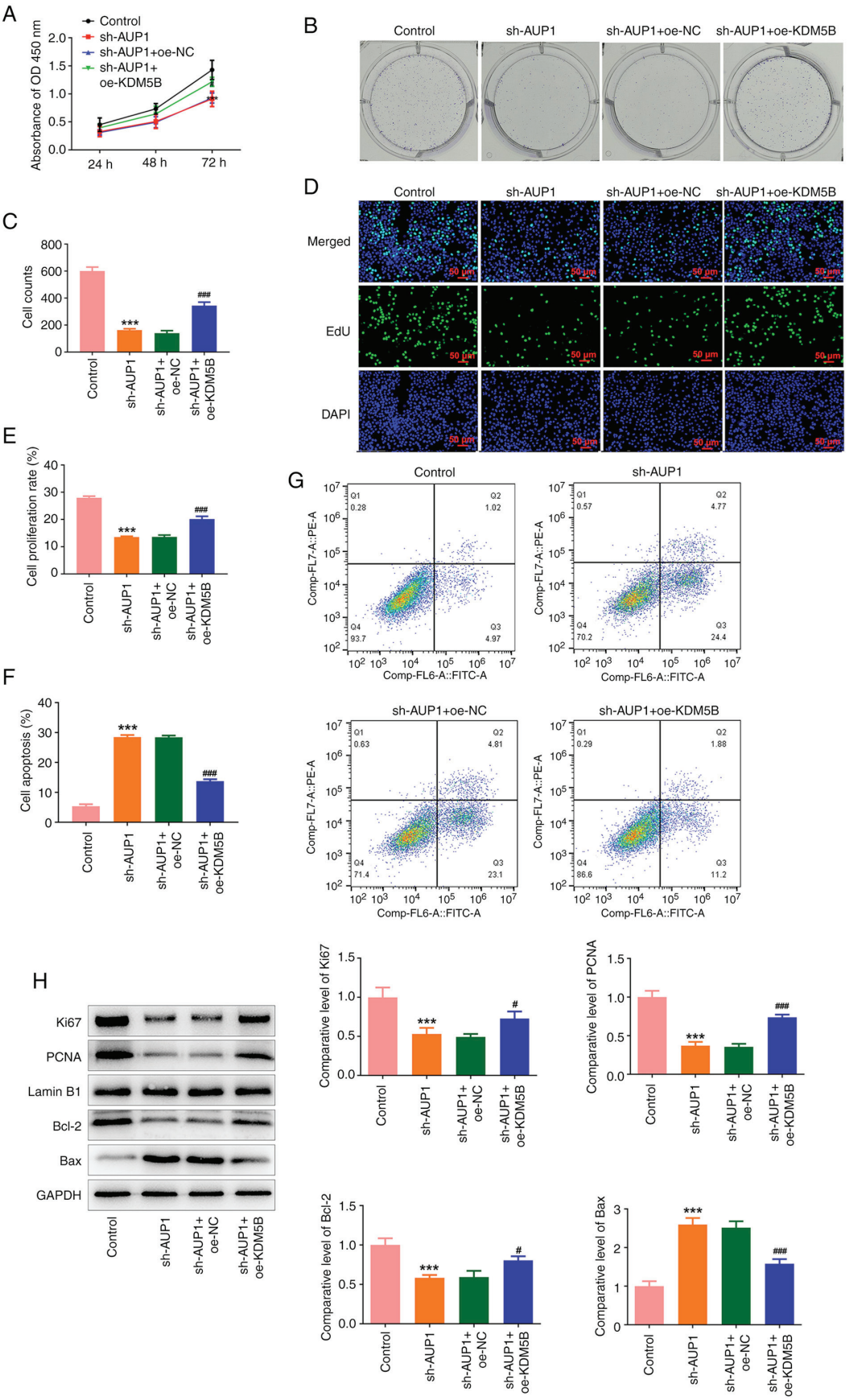

Figure 7. KDM5B overexpression blocks the inhibitory effects of AUP1 silencing on the proliferation and apoptosis of cervical cancer cells. (A) Cell Counting Kit-8 assay was used to measure the viability of SiHa cells. (B and C) Cell proliferation was detected by colony formation assay. (D and E) EdU staining was used to detect the proliferation of SiHa cells. (F and G) SiHa cell apoptosis was detected using flow cytometric analysis. (H) Western immunoblot analysis was used to measure Ki67, PCNA, Bcl-2 and Bax expression in SiHa cells. ***P<0.001 vs. control group; $^{\#}$P<0.05 and $^{\#\#\#}$P<0.001 vs. sh-AUP1 + oe-NC group. KDM5B, lysine demethylase 5B; AUP1, ancient ubiquitous protein 1; dU, 5-ethynyl-2'-deoxyuridine; PCNA, proliferating cell nuclear antigen; sh-, short hairpin; NC, negative control; oe-overexpressing.

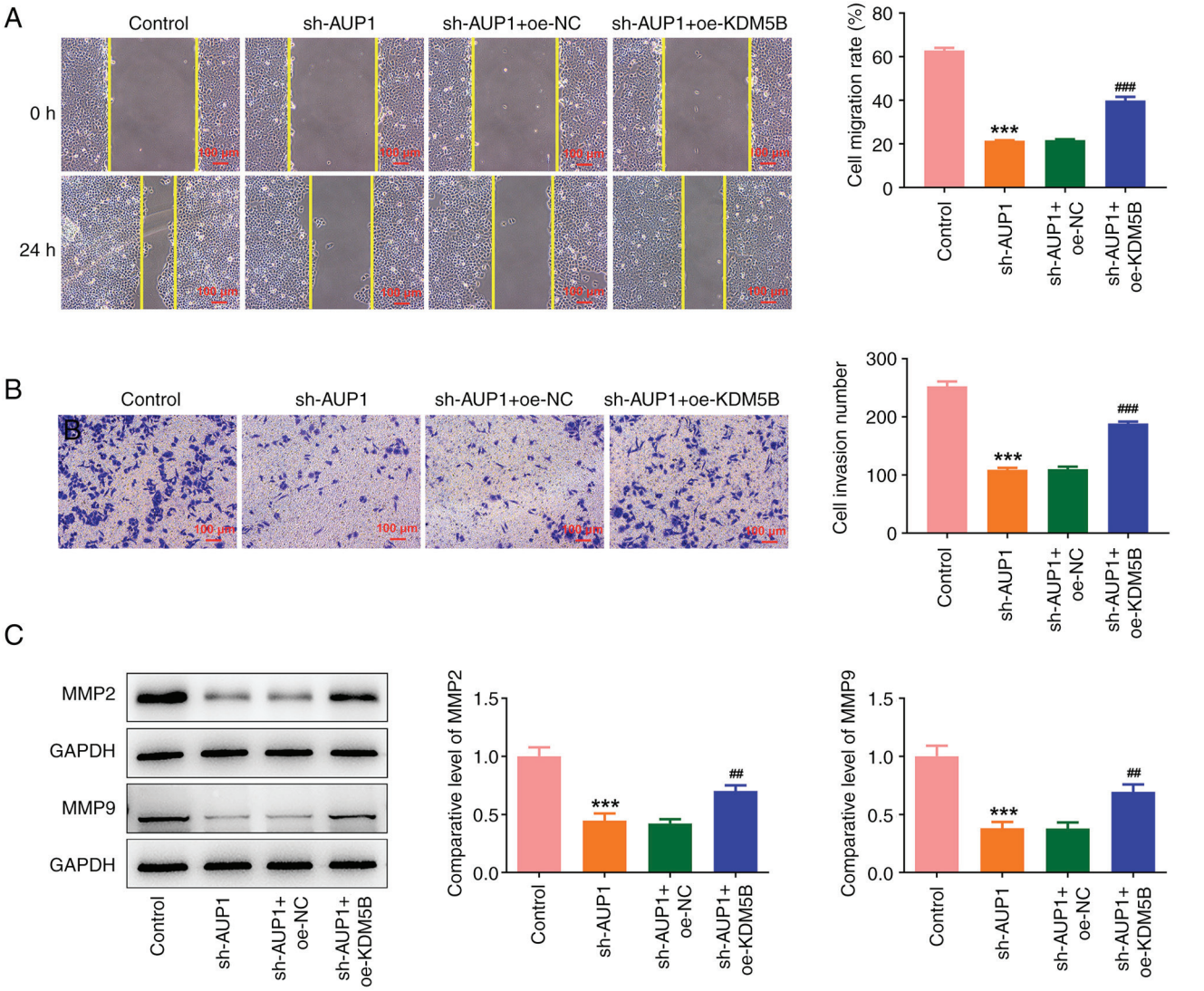

Figure 8. KDM5B overexpression blocks the inhibitory effects of AUP1 silencing on the migration and invasion of cervical cancer cells. (A) Wound healing assay was used to detect the migration of SiHa cells. (B) The invasion of SiHa cells was identified using Transwell assay. (C) Western immunoblot analysis was used to evaluate MMP2 and MMP9 expression in SiHa cells. ***P<0.001 vs. control group; $^{\#\#}$P<0.01 and $^{\#\#\#}$P<0.001 vs. sh-AUP1 + oe-NC group. KDM5B, lysine demethylase 5B; AUP1, ancient ubiquitous protein 1; MMP, matrix metalloproteinase; sh-, short hairpin; NC, negative control; oe-overexpressing.

At the same time, KDM5B overexpression in AUP1-silenced SiHa cells increased Ki67, PCNA and Bcl-2 expression whereas decreased Bax expression (Fig. 7H). Concurrently, the migration and invasion of SiHa cells co-transfected with sh-AUP1 and oe-KDM5B were increased, accompanied by upregulated MMP2 and MMP9 expression (Fig. 8A-C). Collectively, KDM5B transcriptionally activated AUP1 to promote the malignant biological behaviors of cervical cancer cells.

KDM5B overexpression abolishes the impacts of AUP1 silencing on the lipid metabolism reprogramming of cervical cancer cells. The lipid metabolism in SiHa cells was detected following the co-transfection of oe-KDM5B and sh-AUP1. As shown in Fig. 9A-C, KDM5B upregulation led to increased lipid droplets in SiHa cells in sh-AUP1 + oe-KDM5B group compared with the sh-AUP1 + oe-NC group, accompanied by the higher TG and CHOL contents. Meantime, the OCR level in SiHa cells transfected with sh-AUP1 was increased by KDM5B overexpression (Fig. 9D). The results of western immunoblot analysis indicated the downregulated CPT1A, STARD5, PRKAA2 expression and the upregulated MGLL expression in SiHa cells co-transfected with sh-AUP1 and oe-KDM5B (Fig. 9E). These results demonstrated that KDM5B transcriptionally activated AUP1 to reprogram the lipid metabolism of cervical cancer cells.

AUP1 knockdown transcriptionally regulated by KDM5B interferes with the tumor growth and suppresses the lipid metabolism reprogramming in vivo. The SiHa tumor-bearing mice model was established to study the role of AUP1 and KDM5B *in vivo*. The appearance of mice and tumor is demonstrated in Fig. 10A. The injection of SiHa cells with sh-AUP1 significantly decreased the tumor size compared with the control group (Fig. 10B). On the contrary, nude mice injected with sh-AUP1 + oe-KDM5B-expressing SiHa cells showed significantly increased tumor size. Western immunoblot analysis indicated that AUP1 expression

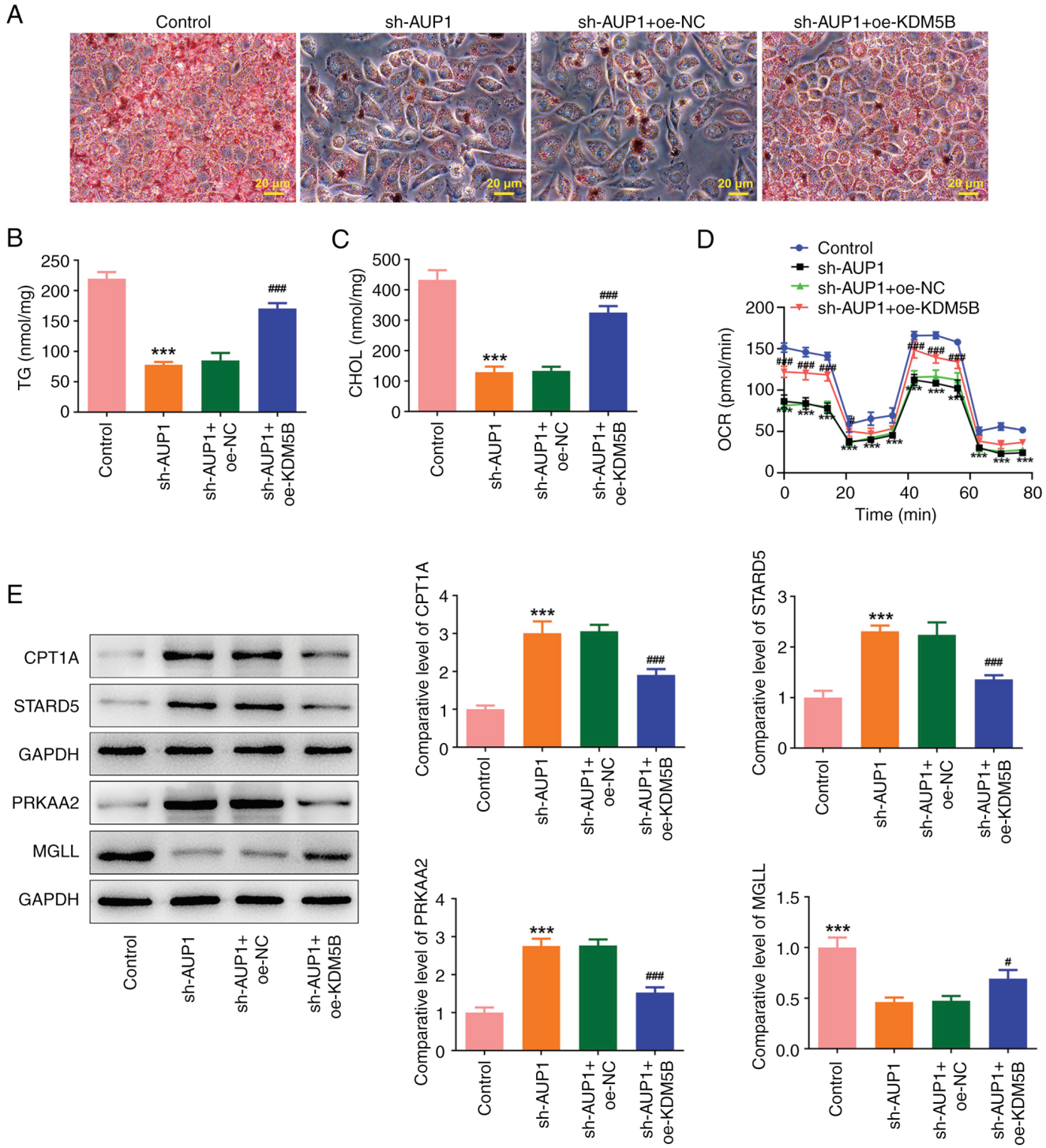

Figure 9. KDM5B overexpression abolishes the impacts of AUP1 silencing on the lipid metabolism reprogramming of cervical cancer cells. (A) Oil red O staining was used to detect lipid droplets in SiHa cells. The contents of (B) TG and (C) CHOL in SiHa cells were analyzed using the corresponding kits. (D) OCR level in SiHa cells was detected using the Seahorse XF Cell Mito Stress Test Kit. (E) The expression of proteins related to lipid metabolism was detected using western immunoblot analysis. ***P<0.001 vs. control group; $^{\#}$P<0.05 and $^{\#\#\#}$P<0.001 vs. sh-AUP1 + oe-NC group. KDM5B, lysine demethylase 5B; AUP1, ancient ubiquitous protein 1; TG, triglyceride; CHOL, cholesterol; OCR, oxygen consumption rates; sh-, short hairpin; NC, negative control; oe-overexpressing.

in tumor tissues was significantly downregulated in the sh-AUP1 group, which was restored by the further KDM5B overexpression (Fig. 10C). Meanwhile, AUP1 knockdown had no significant effect on KDM5B expression (Fig. 10C). On the contrary, compared with the sh-AUP1 + oe-NC group, KDM5B overexpression significantly elevated KDM5B expression in tumor tissues of SiHa tumor-bearing mice. Besides, decreased Ki67 expression and increased TUNEL-positive cells were found in the tumor tissues of mice with AUP1 knockdown, which were then reversed by KDM5B overexpression (Fig. 10D and E). Moreover, lipid droplets in tumor tissues were identified using oil

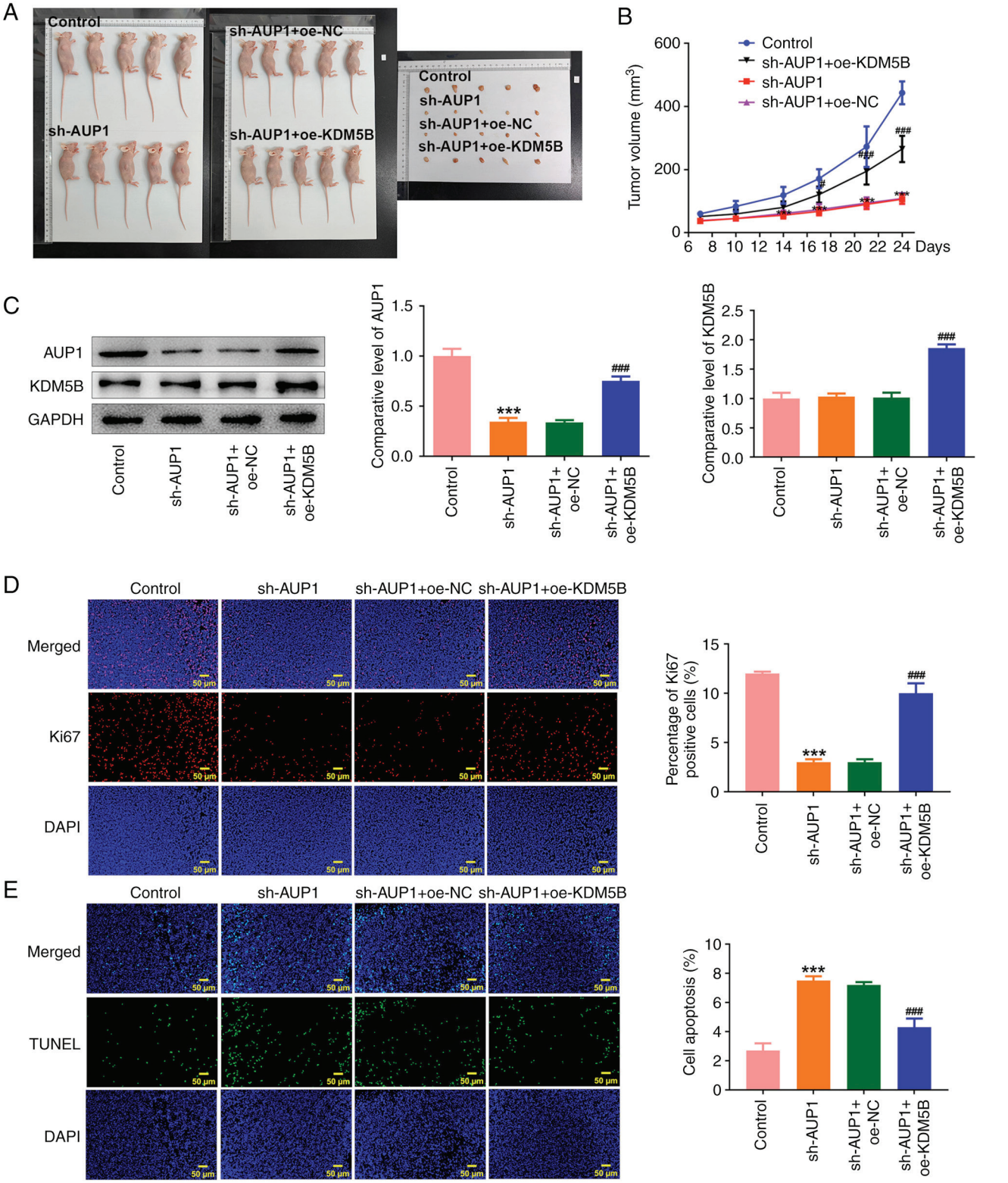

Figure 10. AUP1 knockdown transcriptionally regulated by KDM5B interferes with the tumor growth *in vivo*. (A) The images of SiHa tumor-bearing mice and the dissected tumor. (B) The tumor volumes were recorded every two days from the 6th day after injection. (C) The expression of AUP1 and KDM5B was detected using western immunoblot analysis. (D) Ki67 expression in tumor tissues was detected by immunofluorescence staining. (E) Apoptosis was detected using TUNEL staining. ***P<0.001 vs. control group; $^{\#}$P<0.05 and $^{\#\#\#}$P<0.001 vs. sh-AUP1 + oe-NC group. AUP1, ancient ubiquitous protein 1; KDM5B, lysine demethylase 5B; sh-, short hairpin; NC, negative control; oe-overexpressing.

red O staining. It could be observed that lipid droplets were decreased in the sh-AUP1 group compared with the control group, accompanied by increased CPT1A, STARD5, PRKAA2 expression and decreased MGLL expression (Fig. 11A and B). Compared with the sh-AUP1 + oe-NC group, KDM5B overexpression promoted the lipid accumulation, which was also supported by downregulated CPT1A, STARD5, PRKAA2 expression and upregulated

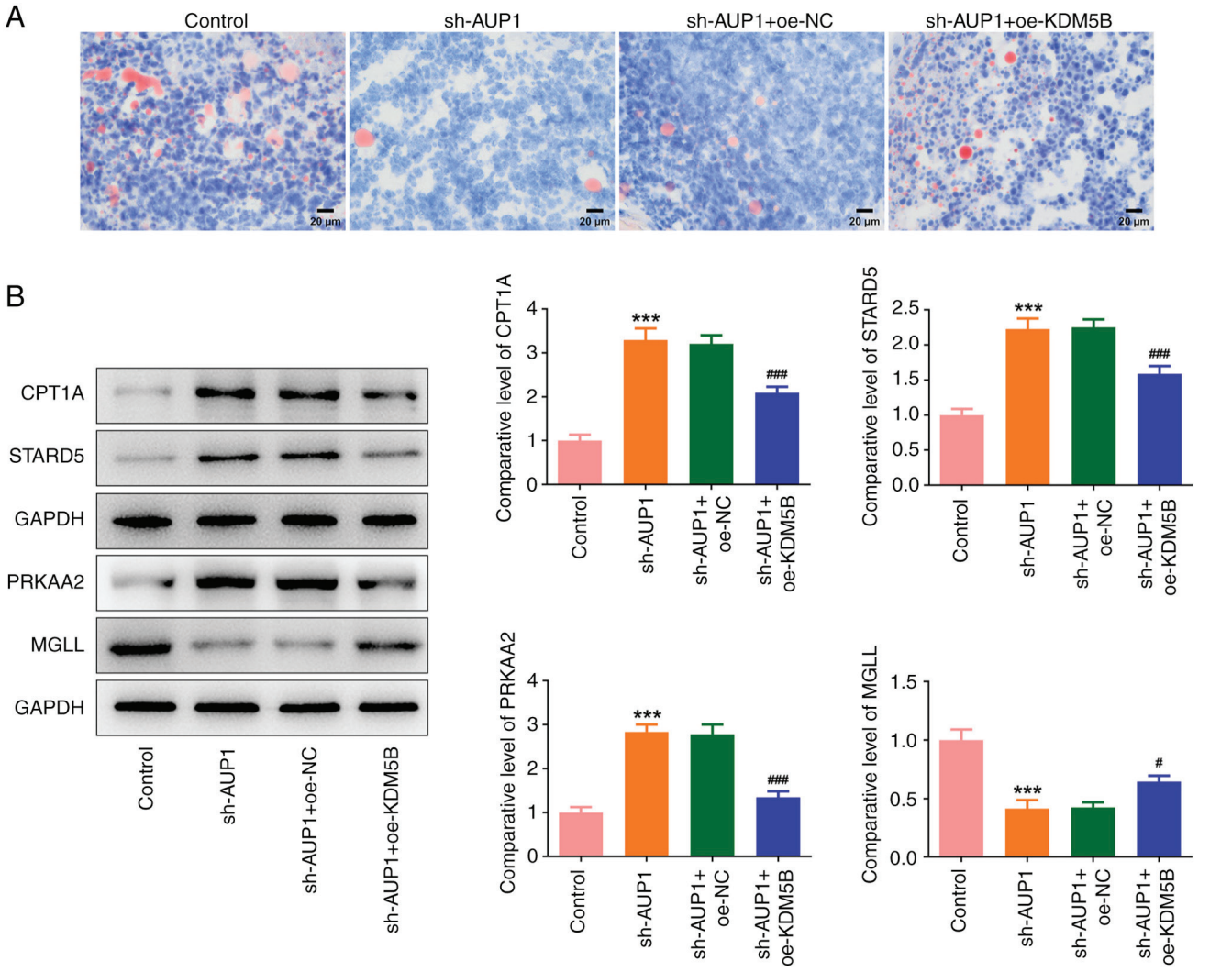

Figure 11. AUP1 knockdown transcriptionally regulated by KDM5B suppresses the lipid metabolism reprogramming *in vivo*. (A) Oil red O staining was used to detect the lipid accumulation in tumor tissues. (B) The expression of proteins related to lipid metabolism in tumor tissues was detected using western immunoblot analysis. ***P<0.001 vs. control group; $^{\#}$P<0.05 and $^{\#\#\#}$P<0.001 vs. sh-AUP1 + oe-NC group. AUP1, ancient ubiquitous protein 1; KDM5B, lysine demethylase 5B; sh-, short hairpin; NC, negative control; oe-overexpressing; CPT1A, carnitine palmitoyltransferase IA; STARD5, StAR-related lipid transfer domain containing 5; MGLL, monoglyceride lipase.

MGLL expression. Collectively, the aforementioned results suggested that AUP1 knockdown transcriptionally regulated by KDM5B interfered with the tumor growth and suppressed the lipid metabolism reprogramming *in vivo*.

Discussion

The present study suggested the abnormally high expression of AUP1 in cervical cancer tissues and cells. AUP1 could be transcriptionally activated by KDM5B to reprogram lipid metabolism, thereby promoting the malignant progression of cervical cancer. The present findings provided mechanistic insights and more rationales for developing new cervical cancer therapies.

AUP1, a lipid droplet-localized type-III membrane protein, was initially recognized and defined by Meisler *et al* in 1996 (13). A recent study has reported that AUP1 expression is increased in glioblastoma tumor component and AUP1 expression is correlated with tumor grade (31). As one of the lipid droplet-associated genes, AUP1 has been regarded as a diagnostic and prognostic biomarker in head and neck squamous cell carcinoma (32). Importantly, Chen *et al* (15) revealed the abnormally high AUP1 expression in clinical samples of patients with renal clear cell carcinoma, and they also demonstrated that AUP1 deficiency could inhibit the proliferation, migration and invasion of renal clear cell carcinoma *in vitro* and *in vivo*. In terms of uveal melanoma, AUP1 interference restrains the proliferation and invasion of uveal melanoma cells (33). In the present study, highly expressed AUP1 was found in the cervical cancer tissues and cell lines, and higher AUP1 expression in patients with cervical cancer was associated with poorer prognosis, which is consistent with previous studies on the significance of AUP1 expression in other tumors aforementioned. It is already known that tumor cells have malignant characteristics of infinite proliferation, migration, invasion and apoptosis resistance in the process of malignant transformation (34-36). Functional experiments suggested that AUP1

interference inhibited these malignant biological behaviors of cervical cancer cells, suggesting the anti-cervical cancer potential of AUP1 knockdown.

The metabolic system of cells plays a major regulatory role in maintaining the rapid proliferation and strong activity of tumor cells. In recent years, lipid metabolic disorders have become increasingly important in terms of tumor cell metabolism (37). Lipid metabolism is highly reprogrammed in cancer cells to meet altered energy requirements caused by elevated membrane structure formation during the rapid proliferation, mainly manifested as increased lipid production, lipid storage of intracellular lipid droplets and changed expression of related genes (38). Targeting altered lipid metabolism in cancer cells has been considered to be a promising strategy for cancer therapy (39). In cervical cancer, Linc00657 promotes Skp2 expression to facilitate the cancer progression by reprogramming fatty acid metabolism (40). As a lipid metabolism regulator, HSDL2 modulates the proliferation, migration and invasion of cervical cancer cells (40). It has been reported that the decrease in lipid levels (TG and CHOL) significantly attenuates the energy supply and biofilm synthesis to maintain cell proliferation (41). There are a variety of enzymes involved in the regulation of lipid metabolism in cancer cells. For instance, CPT1A is a key rate-limiting enzyme for fatty acid oxidation, and increased CPT1A expression can inhibit lipid deposition (42). STARD5 is a lipid transporter that participates in the lipid transport between different cell membranes (43). Insufficiency of STARD5 displays not only liver triglyceride accumulation but also dysregulation in genes of the fatty acid synthesis pathway (44). As previously reported, PRKAA2 is a crucial energy-sensing enzyme that can monitor cellular energy status, which can phosphorylate and inactivate acetyl-CoA carboxylase, thereby inhibiting the *de novo* synthesis of fatty acid (30). Besides, as a key metabolic enzyme in lipid metabolism, MGLL is responsible for the conversion of triglycerides into free fatty acids (45). AUP1 localizes to lipid droplets and AUP1 expression level affects the accumulation of lipid droplets in cells (46). The increased accumulation of lipid droplets is an important hallmark of neck squamous cell carcinoma, and AUP1 is found to be a differentially expressed lipid droplet-associated gene with diagnostic and prognostic potential in neck squamous cell carcinoma (32). Particularly, AUP1 can directly interfere with tumor progression by modulating lipid metabolism and inducing lipid accumulation (15). In the present study, AUP1 interference inhibited the lipid metabolism reprogramming of cervical cancer cells, as evidenced by reduced lipid droplets disposition, TG and CHOL contents and OCR level, increased CPT1A, STARD5 and PRKAA2 expression and decreased MGLL expression in SiHa cells.

KDM5B was predicted to be one of the upstream transcription factors that could transcriptionally regulate AUP1 expression, which was confirmed by luciferase reporter assay and ChIP assay in the present study. As an oncogene, KDM5B is closely related to tumorigenesis and targeting KDM5B has emerged as a promising strategy for cancer treatment (47). KDM5B expression has been observed to be significantly increased in cervical cancer and the loss of KDM5B function suppresses the growth of cervical cancer cells (19). KDM5B is a new regulator involved in lipid metabolism and KDM5B participates in diabetic peripheral neuropathy by regulating SIRT3-mediated mitochondrial glycolipid metabolism (48). Moreover, Backe *et al* (49) have highlighted the role of KDM5B in glucose metabolic homeostasis. KDM5B has been found to promote the malignant progression of breast cancer by regulating lipid metabolism reprogramming, and KDM5B deficiency can reregulate the levels of lipid metabolizing enzymes in breast cancer cells (18). Consistent with the aforementioned studies, KDM5B was highly expressed in SiHa cells, and KDM5B overexpression abolished the impacts of AUP1 downregulation on the malignant biological behaviors and lipid metabolism reprogramming of cervical cancer cells, which were further supported by the *in vivo* experiments in SiHa tumor-bearing mice. These results together demonstrated that AUP1 transcriptionally activated by KDM5B reprogramed lipid metabolism to accelerate the malignant progression of cervical cancer.

However, the present study had a limitation. AUP1 expression was only evaluated in cervical cancer tissues through bioinformatics tools. The analysis of clinical cervical cancer tissue samples will be included in our future investigation.

In conclusion, the present study was the first to reveal the upregulation of AUP1 expression in cervical cancer tissues and cells. The functional analysis experiments proved that AUP1 could be transcriptionally activated by KDM5B to reprogram lipid metabolism, thereby promoting the malignant progression of cervical cancer. The results of the present study may provide mechanistic insights and reveal possible therapeutic strategies in targeting metabolic pathways.

Acknowledgements

Not applicable.

Funding

The present study was supported by the National Natural Science Foundation of China (grant no. 82305292), the Zhejiang Provincial Medical and Health Science and Technology Plan Project (grant no. 2023KY854) and the Zhejiang University Students Science and Technology Innovation Activity Plan (grant no. 2024R410B060).

Availability of data and materials

The data generated in the present study may be requested from the corresponding author.

Authors' contributions

YZ and MC contributed to the conception and design of the present study. YZ, WY and XW analyzed the data and drafted the manuscript. WY and MC contributed to make the figures. All authors participated in the experiments. MC reviewed and edited the manuscript. All authors read and approved the final version of the manuscript. YZ and MC confirm the authenticity of all the raw data.

Ethics approval and consent to participate

The animal experiments were approved by the Laboratory Animal Ethics Committee of The First Affiliated Hospital of Zhejiang Chinese Medical University (approval no. HB2005007; Hangzhou, China).

Patient consent for publication

Not applicable.

Competing interests

The authors declare that they have no competing interests.

References

1. Siegel RL, Miller KD, Fuchs HE and Jemal A: Cancer statistics, 2022. CA Cancer J Clin 72: 7-33, 2022.
2. Sung H, Ferlay J, Siegel RL, Laversanne M, Soerjomataram I, Jemal A and Bray F: Global cancer statistics 2020: GLOBOCAN estimates of incidence and mortality worldwide for 36 cancers in 185 countries. CA Cancer J Clin 71: 209-249, 2021.
3. Xia C, Dong X, Li H, Cao M, Sun D, He S, Yang F, Yan X, Zhang S, Li N and Chen W: Cancer statistics in China and United States, 2022: Profiles, trends, and determinants. Chin Med J (Engl) 135: 584-590, 2022.
4. Walboomers JM, Jacobs MV, Manos MM, Bosch FX, Kummer JA, Shah KV, Snijders PJ, Peto J, Meijer CJ and Muñoz N: Human papillomavirus is a necessary cause of invasive cervical cancer worldwide. J Pathol 189: 12-19, 1999.
5. Nakisige C, Trawin J, Mitchell-Foster S, Payne BA, Rawat A, Mithani N, Amuge C, Pedersen H, Orem J, Smith L and Ogilvie G: Integrated cervical cancer screening in Mayuge District Uganda (ASPIRE Mayuge): A pragmatic sequential cluster randomized trial protocol. BMC Public Health 20: 142, 2020.
6. Kubik J, Humeniuk E, Adamczuk G, Madej-Czerwonka B and Korga-Plewko A: Targeting energy metabolism in cancer treatment. Int J Mol Sci 23: 5572, 2022.
7. Cheng C, Geng F, Cheng X and Guo D: Lipid metabolism reprogramming and its potential targets in cancer. Cancer Commun (Lond) 38: 27, 2018.
8. Broadfield LA, Pane AA, Talebi A, Swinnen JV and Fendt SM: Lipid metabolism in cancer: New perspectives and emerging mechanisms. Dev Cell 56: 1363-1393, 2021.
9. Luo X, Cheng C, Tan Z, Li N, Tang M, Yang L and Cao Y: Emerging roles of lipid metabolism in cancer metastasis. Mol Cancer 16: 76, 2017.
10. Han C, Hu C, Liu T, Sun Y, Hu F, He Y, Zhang J, Chen J, Ding J, Fan J, *et al*: IGF2BP3 enhances lipid metabolism in cervical cancer by upregulating the expression of SCD. Cell Death Dis 15: 138, 2024.
11. Yang Y, Han A, Wang X, Yin X, Cui M and Lin Z: Lipid metabolism regulator human hydroxysteroid dehydrogenase-like 2 (HSDL2) modulates cervical cancer cell proliferation and metastasis. J Cell Mol Med 25: 4846-4859, 2021.
12. Ping P, Li J, Lei H and Xu X: Fatty acid metabolism: A new therapeutic target for cervical cancer. Front Oncol 13: 1111778, 2023.
13. Jang W, Weber JS, Bashir R, Bushby K and Meisler MH: Aup1, a novel gene on mouse chromosome 6 and human chromosome 2p13. Genomics 36: 366-368, 1996.
14. Robichaud S, Fairman G, Vijithakumar V, Mak E, Cook DP, Pelletier AR, Huard S, Vanderhyden BC, Figeys D, Lavallée-Adam M, *et al*: Identification of novel lipid droplet factors that regulate lipophagy and cholesterol efflux in macrophage foam cells. Autophagy 17: 3671-3689, 2021.
15. Chen C, Zhao W, Lu X, Ma Y, Zhang P, Wang Z, Cui Z and Xia Q: AUP1 regulates lipid metabolism and induces lipid accumulation to accelerate the progression of renal clear cell carcinoma. Cancer Sci 113: 2600-2615, 2022.
16. Xhabija B and Kidder BL: KDM5B is a master regulator of the H3K4-methylome in stem cells, development and cancer. Semin Cancer Biol 57: 79-85, 2019.
17. Jose A, Shenoy GG, Sunil Rodrigues G, Kumar NAN, Munisamy M, Thomas L, Kolesar J, Rai G, Rao PPN and Rao M: Histone demethylase KDM5B as a therapeutic target for cancer therapy. Cancers (Basel) 12: 2121, 2020.
18. Zhang ZG, Zhang HS, Sun HL, Liu HY, Liu MY and Zhou Z: KDM5B promotes breast cancer cell proliferation and migration via AMPK-mediated lipid metabolism reprogramming. Exp Cell Res 379: 182-190, 2019.
19. Zhou Y, An Q, Guo RX, Qiao YH, Li LX, Zhang XY and Zhao XL: miR424-5p functions as an anti-oncogene in cervical cancer cell growth by targeting KDM5B via the Notch signaling pathway. Life Sci 171: 9-15, 2017.
20. Chandrashekar DS, Bashel B, Balasubramanya SAH, Creighton CJ, Ponce-Rodriguez I, Chakravarthi BVSK and Varambally S: UALCAN: A portal for facilitating tumor subgroup gene expression and survival analyses. Neoplasia 19: 649-658, 2017.
21. Lacny S, Wilson T, Clement F, Roberts DJ, Faris P, Ghali WA and Marshall DA: Kaplan-Meier survival analysis overestimates cumulative incidence of health-related events in competing risk settings: A meta-analysis. J Clin Epidemiol 93: 25-35, 2018.
22. Hu H, Miao YR, Jia LH, Yu QY, Zhang Q and Guo AY: AnimalTFDB 3.0: A comprehensive resource for annotation and prediction of animal transcription factors. Nucleic Acids Res 47 (D1): D33-D38, 2019.
23. Livak KJ and Schmittgen TD: Analysis of relative gene expression data using real-time quantitative PCR and the 2(-Delta Delta C(T)) method. Methods 25: 402-408, 2001.
24. Shay G, Lynch CC and Fingleton B: Moving targets: Emerging roles for MMPs in cancer progression and metastasis. Matrix Biol 44-46: 200-206, 2015.
25. Sun YS, Thakur K, Hu F, Cespedes-Acuña CL, Zhang JG and Wei ZJ: Icariside II suppresses cervical cancer cell migration through JNK modulated matrix metalloproteinase-2/9 inhibition in vitro and in vivo. Biomed Pharmacother 125: 110013, 2020.
26. Xu S, Fan Y, Li D, Liu Y and Chen X: Glycoprotein nonmetastatic melanoma protein B accelerates tumorigenesis of cervical cancer in vitro by regulating the Wnt/β-catenin pathway. Braz J Med Biol Res 52: e7567, 2018.
27. Maan M, Peters JM, Dutta M and Patterson AD: Lipid metabolism and lipophagy in cancer. Biochem Biophys Res Commun 504: 582-589, 2018.
28. Li A, Qin Y, Zhang Y, Zhen X and Gong G: Evaluation of oxygen consumption rates in situ. Methods Mol Biol 2755: 215-226, 2024.
29. Jung YY, Kim HM and Koo JS: Expression of lipid metabolism-related proteins in metastatic breast cancer. PLoS One 10: e0137204, 2015.
30. Snaebjornsson MT, Janaki-Raman S and Schulze A: Greasing the wheels of the cancer machine: The role of lipid metabolism in cancer. Cell Metab 31: 62-76, 2020.
31. Chang PC, Lin YC, Yen HJ, Hueng DY, Huang SM and Li YF: Ancient ubiquitous protein 1 (AUP1) is a prognostic biomarker connected with TP53 mutation and the inflamed microenvironments in glioma. Cancer Cell Int 23: 62, 2023.
32. Bai YT, Wang X, He MJ, Xie JR, Chen XJ and Zhou G: The potential of lipid droplet-associated genes as diagnostic and prognostic biomarkers in head and neck squamous cell carcinoma. Comb Chem High Throughput Screen 27: 136-147, 2024.
33. Liu J, Zhang P, Yang F, Jiang K, Sun S, Xia Z, Yao G and Tang J: Integrating single-cell analysis and machine learning to create glycosylation-based gene signature for prognostic prediction of uveal melanoma. Front Endocrinol (Lausanne) 14: 1163046, 2023.
34. Novikov NM, Zolotaryova SY, Gautreau AM and Denisov EV: Mutational drivers of cancer cell migration and invasion. Br J Cancer 124: 102-114, 2021.
35. Zheng HC, Xue H and Zhang CY: REG4 promotes the proliferation and anti-apoptosis of cancer. Front Cell Dev Biol 10: 1012193, 2022.
36. Li Z, He H, Ren X, Chen Y, Liu W, Pu R, Fang L, Shi Y, Liu D, Zhao J, *et al*: APOBEC3A suppresses cervical cancer via apoptosis. J Cancer 14: 3429-3443, 2023.
37. Pascual G, Majem B and Benitah SA: Targeting lipid metabolism in cancer metastasis. Biochim Biophys Acta Rev Cancer 1879: 189051, 2024.
38. Bacci M, Lorito N, Smiriglia A and Morandi A: Fat and furious: Lipid metabolism in antitumoral therapy response and resistance. Trends Cancer 7: 198-213, 2021.

39. Wang Z, Wang Y, Li Z, Xue W, Hu S and Kong X: Lipid metabolism as a target for cancer drug resistance: Progress and prospects. Front Pharmacol 14: 1274335, 2023.
40. Li Y, Maimaitirexiati G, Wang J, Zhang J, Tian P, Zhou C, Ren J, Wang L, Zhao J, Wang H, *et al*: Long non-coding RNA Linc00657 up-regulates Skp2 to promote the progression of cervical cancer through lipid reprogramming and regulation of immune microenvironment. Cytokine 176: 156510, 2024.
41. Blank HM, Papoulas O, Maitra N, Garge R, Kennedy BK, Schilling B, Marcotte EM and Polymenis M: Abundances of transcripts, proteins, and metabolites in the cell cycle of budding yeast reveal coordinate control of lipid metabolism. Mol Biol Cell 31: 1069-1084, 2020.
42. Schlaepfer IR and Joshi M: CPT1A-mediated fat oxidation, mechanisms, and therapeutic potential. Endocrinology 161: bqz046, 2020.
43. Alpy F and Tomasetto C: Give lipids a START: The StAR-related lipid transfer (START) domain in mammals. J Cell Sci 118: 2791-2801, 2005.
44. Kakiyama G, Minoiwa K, Bai-Kamara N, Hashiguchi T, Pandak WM and Rodriguez-Agudo D: StarD5 levels of expression correlate with onset and progression of steatosis and liver fibrosis. Am J Physiol Gastrointest Liver Physiol 326: G747-G761, 2024.
45. Zhang J, Song Y, Shi Q and Fu L: Research progress on FASN and MGLL in the regulation of abnormal lipid metabolism and the relationship between tumor invasion and metastasis. Front Med 15: 649-656, 2021.
46. Klemm EJ, Spooner E and Ploegh HL: Dual role of ancient ubiquitous protein 1 (AUP1) in lipid droplet accumulation and endoplasmic reticulum (ER) protein quality control. J Biol Chem 286: 37602-37614, 2011.
47. Fu YD, Huang MJ, Guo JW, You YZ, Liu HM, Huang LH and Yu B: Targeting histone demethylase KDM5B for cancer treatment. Eur J Med Chem 208: 112760, 2020.
48. Jiao Y, Li YZ, Zhang YH, Cui W, Li Q, Xie KL, Yu Y and Yu YH: Lysine demethylase KDM5B down-regulates SIRT3-mediated mitochondrial glucose and lipid metabolism in diabetic neuropathy. Diabet Med 40: e14964, 2023.
49. Backe MB, Jin C, Andreone L, Sankar A, Agger K, Helin K, Madsen AN, Poulsen SS, Bysani M, Bacos K, *et al*: The lysine demethylase KDM5B regulates islet function and glucose homeostasis. J Diabetes Res 2019: 5451038, 2019.